Implant Stability and Bone Remodeling after 3 and 13 Days of Implantation with an Initial Static Strain

Anders Halldin, MSc (PhD student);[*†] Ryo Jimbo, DDS, PhD;[‡] Carina B. Johansson, PhD;[§] Ann Wennerberg, DDS, PhD;[¶] Magnus Jacobsson, MD, PhD;[**,††] Tomas Albrektsson, MD, PhD, ODHc;[‡‡,§§] Stig Hansson, PhD[¶¶]

ABSTRACT

Objective: Bone is constantly exposed to dynamic and static loads, which induce both dynamic and static bone strains. Although numerous studies exist on the effect of dynamic strain on implant stability and bone remodeling, the effect of static strain needs further investigation. Therefore, the effect of two different static bone strain levels on implant stability and bone remodeling at two different implantation times was investigated in a rabbit model.

Methods: Two different test implants with a diametrical expansion of 0.15 mm (group A) and 0.05 mm (group B) creating initial static bone strains of 0.045 and 0.015, respectively. The implants were inserted in the proximal tibial metaphysis of 24 rabbits to observe the biological response at implant removal. Both groups were compared to control implants (group C), with no diametrical increase. The insertion torque (ITQ) was measured to represent the initial stability and the removal torque (RTQ) was measured to analyze the effect that static strain had on implant stability and bone remodeling after 3 and 13 days of implantation time.

Results: The ITQ and the RTQ values for test implants were significantly higher for both implantation times compared to control implants. A selection of histology samples was prepared to measure bone to implant contact (BIC). There was a tendency that the BIC values for test implants were higher compared to control implants.

Conclusion: These findings suggest that increased static bone strain creates higher implant stability at the time of insertion, and this increased stability is maintained throughout the observed period.

KEY WORDS: animal model, bone resorption, implant stability

INTRODUCTION

It is widely accepted that mechanical stimuli alter the mass and structure of bone. The load induces strain in the bone that affects the modeling and remodeling processes to adapt the bone to the load that it is exposed to. It has been reported that these modeling and remodeling processes are dependent on strain magnitude, strain frequency, strain rate, and duration,[1–7] and it is suggested that dynamic strains are the driving factor behind modeling and remodeling.[6] In a study on roosters, Rubin and Lanyon found that application of 36 cycles at 0.5 Hz per day for 6 weeks with a strain level of ~2,000 μ strain on ulna showed an increase in bone mass compared to application of 4 cycles per day.[5] Another study in rats concluded that lower strain required more cycles to activate bone modeling.[1] Interestingly, only a few

*Researcher, Department of Prosthodontics, Faculty of Odontology, Malmö University, Malmö, Sweden; †researcher, Astra Tech AB, Mölndal, Sweden; ‡associated professor, Department of Prosthodontics, Faculty of Odontology, Malmö University, Malmö, Sweden; §professor, Department of Prosthodontics/Dental Material Science, Institute of Odontology, The Sahlgrenska Academy, University of Gothenburg, Göteborg, Sweden; ¶professor, Department of Prosthodontics, Faculty of Odontology, Malmö University, Malmö, Sweden; **professor, Department of Prosthodontics, Faculty of Odontology, Malmö University, Malmö, Sweden; ††vice president, Astra Tech AB, Mölndal, Sweden; ‡‡professor & head, Department of Biomaterials, Gothenburg University, Göteborg, Sweden; §§senior scientist, Department of Dental Materials Sciences & Technology, Malmö University, Sweden; ¶¶senior scientific executive, Research & Development, Astra Tech AB, Mölndal, Sweden

Reprint requests: Mr. Anders Halldin, Department of Prosthodontics, Faculty of Odontology, Malmö University, Malmö, Sweden. e-mail: anders.halldin@mah.se

DOI 10.1111/cid.12000

studies have investigated how static strain affects bone modeling and remodeling.[8–10] Perren and colleagues[10] induced a pressure to intact and osteotomized bone and recorded the change in pressure over time and discovered that the pressure slowly decreases with time. In a study by Lynch and Silva,[9] it was concluded that bone damage created by static strain can trigger woven bone response. Halldin and colleagues[8] demonstrated that static strain induced by a press-fit implant is maintained 24 days after insertion. When an implant is inserted in the bone with a press fit, it induces static strain to the bone. The level of static strain that the bone can withstand before fracture depends on the type of bone,[11,12] degree of mineralization,[13] age,[14] and loading rate.[15] According to Currey,[13] the adult human femur has an ultimate strain level of 0.02 strains and a yield strain level of 0.007. McCalden and colleagues[14] reported ultimate strains, for human femora, ranging from 0.01 to 0.04 with lower values for higher ages. McElhaney[15] demonstrated ultimate strains of human cortical bone in the range of 0.01 to 0.02 with lower values for high strain rates. The yield strain level for various types of bone and species is in the range of 0.005 to 0.01.[13] The magnitude of static strain induced to the bone during implant installation depends on implant geometry, osteotomy preparation, bone anatomy, and surgical technique. Initially, the static strain creates a press fit that stabilizes the implant during the osseointegration and remodeling process. Hence, to understand how the remodeling process alters the prestress over time, it is of great interest to obtain enhanced initial implant stability by increased controlled press fit.

After implant installation, bone modeling and remodeling are initiated to heal the surgical trauma and to increase the implant stability.[16,17] It has been suggested that high strain or compression beyond the physiological limit may result in ischemia and pressure necrosis that may reduce the implant stability during the first few weeks.[18] This has been said to be one of the reasons for the implant failure in clinical situations, where high amount of torque is misinterpreted as high initial stability.[19] An earlier investigation has reported that static strain less than the yield strain seems not to induce rapid bone resorption.[10] In our previous study, it was found that a press fit remained after 24 days in rabbit with an initial static strain beyond the yield strain.[8] It has been suggested that prestressed bone is gradually eliminated during remodeling.[10] In clinical studies, a greater decrease in implant stability after 2–3 weeks has been observed in bone of lower quality.[16] The reduction in stability was explained by remodeling of old bone before new bone formation increases implant stability.[16] In addition, bone is a viscoelastic material[20,21] that reduces the initial prestress due to relaxation of the material, and, hence, mechanically reduces the implant stability over time. The reduction in prestress due to viscoelastic effects is greatest directly after the induced strain.[10,22] The initial reduction of implant stability may partly be explained by the viscoelastic properties of bone. It is of great interest to investigate how different static strains affect the implant stability and bone remodeling during the initial healing phase. The aim of the present study was to investigate the effects of predetermined static strains between the yield strain (~0.007) and ultimate strain (~0.02) and beyond the ultimate strain (~0.02) on implant stability and bone remodeling during the initial healing phase in a rabbit model, represented by the removal torque (RTQ) value 3 and 13 days after implant installation. The static strains were induced during implant insertion, by an increase in implant diameter.

MATERIALS AND METHODS

Implants and Surface Topographical Characterization

Specially designed turned screw-shaped implants of titanium (grade 4), manufactured with tight tolerances and without surface treatments, were used in this study. The test implants comprised of three different portions: one cutting portion, one transition portion with a gradual increase in diameter, and one condensation portion Figure 1. Test implants of group A had an

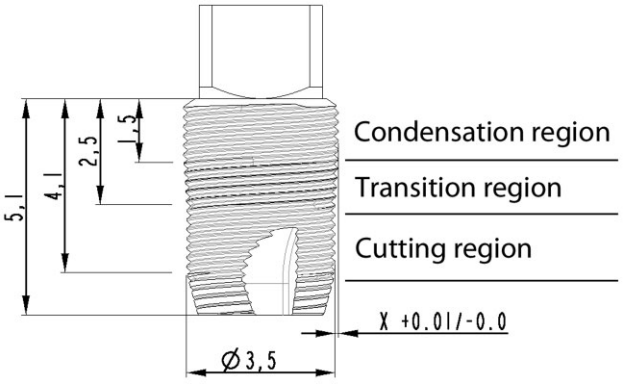

Figure 1 Illustration of the implants with different regions.

increase in diameter from the cutting region to the condensation region of 0.15 mm and test implants of group B had an increase in diameter of 0.05 mm. The test implants were compared to the control implants (group C) which had no diametrical increase.

Surgical Procedures and Insertion Torque

Twenty-four New Zealand white mature rabbits (females, approximately 10 months old) were used in this study. The study was approved by the local animal ethical committee at Gothenburg University. Animals were anesthetized with intramuscular injections of fentanyl and fluanisone (Hypnorm Vet, Janssen Farmaucetica, Belgium) at a dose of 0.5 ml per kg of body weight and intraperitoneal injections of diazepam (Stesolid, Dumex, Denmark) at a dose of 0.25 mg per animal. Before surgery, the rabbits were carefully shaved and washed with a mixture of 70% chlorhexidine and 70% ethanol. Thereafter, local anesthesia with 1.0 ml of 5% lidocaine (Xylocain, AstraZeneca, Södertälje, Sweden) was injected subcutaneously in the surgical site. Each animal received two implants in the proximal tibia metaphysis of each leg. The left leg was used for the test implants (group A and B). Group A implants were installed proximally in the proximal tibia metaphysis and group B implants were installed distally. The control implants (group C) were installed the right leg. The osteotomy was prepared with several drills under constant irrigation of physiological saline solution to a final drill diameter of 3.3 mm corresponding to the core diameter of the cutting portion of the implant. The implants were inserted with the rotation speed set at 25 revolutions/min using W&H implant unit (Elcomed, W&H SA-310, Burmoos, Austria). During installation, the cutting features of the implants created a threaded cavity in the bone, to match the outer shape of the implant. The cutting region defines the shape of the bone before the transitional region gradually increases the strains in the surrounding bone to the final condensation level. The condensation region equalizes the strain in the cortical bone. The installation stopped when the upper section of the condensation region was flushed with the cortical bone surface. The insertion torque (ITQ) was measured by the drilling unit during the installation procedure. The maximum insertion torque represents the torque achieved by the condensation feature. After the surgery, a single dose of prophylactic antibiotic (Borgal, Intervet, Boxmeer, Netherlands) was administered, 0.5 ml per kg body weight.

One animal was euthanized after 10 days due to infection not related to surgery.

RTQ

At 3 days and 13 days after implant installation, the remaining 23 animals were euthanized with an overdose of pentobarbital sodium (60 mg/ml, Apoteksbolaget AB, Stockholm, Sweden). The skin above the implants was incised, and the RTQ was measured on eight animals with 3 days implantation time and on seven animals with 13 days implantation time. The remaining four animals for each implantation time were processed for histologic analysis. The peak RTQ was recorded with a computer control RTQ device, in which the values were transmitted at a frequency of 100 Hz to the computer via a control box.[23] The square-shaped implant head was connected to the RTQ device, and an increasing torque was applied until failure of the bone-implant interface occurred. The maximum torque represents the RTQ value.

Unfortunately, one test implant from group (B) exhibited higher RTQ than what the RTQ device was preset to record as a maximum value. However, the maximum recorded value was used in the statistical calculations.

Preparation of Undecalcified Cut and Ground Sections

In order to comprehend the biological effects of the various static strains, paired samples from four rabbits were randomly chosen for histologic evaluation. In brief, after euthanization, the samples were immersed in 4% neutral buffered formaldehyde, and were subjected to undecalcified cut and ground sectioning[24,25] with the Exakt equipment (Exakt Apparatebau, Norderstedt, Germany). Processing of the samples were initiated by dehydration in ethanol from 70% up to 100% followed by infiltration in diluted resins and finally embedding in pure resin (Technovit 7200 VLC, Kulzer, Germany). Thereafter, the samples were cured using UV light. The cured blocks were divided in the long axis of the implant and one central 200-µm section from each implant was prepared. The sections were ground with SiC papers of various grain sizes to a final thickness of 15 µm. The sections were stained with the routine staining, that is, toluidine blue mixed in pyronin G allowing identification of

bone to implant contact (BIC) using a light microscope. Finally, the section was coverslipped with ordinary mounting media before histomorphometrical.

Histologic Observations

The prepared sections were subjected to histomorphometric analyses. The BIC was quantified using a light microscope (Eclipse ME600, Nikon, Japan) and software (Image J 1.45 S, Wayne Rasband, National Institute of Health, USA). The BIC was defined as the distance of BIC in µm between two thread speaks just below the cortical bone. To be included in the measurement, two thread speaks had to be located in the condensed region.

Statistical Analysis

Analyses of changes in RTQ, ITQ, and BIC between test (A and B) and control (C) implants within the same implantation time were performed using pairwise *t*-tests. The data were assumed to be normally distributed after performing standard statistical tests for normality. Analyses of changes in RTQ over time (24 days data were extracted from previous study) were performed using two-sample *t*-tests. Again, data were assumed to be normally distributed after performing standard statistical tests for normality.

Theoretical Calculations

In an earlier study by Halldin and colleagues,[8] a two-dimensional axisymmetric FEA simulation of the condensation process was performed to calculate the theoretical maximum principal strain induced by a radial displacement of the implant surface of 0.075 mm representing group A and 0.025 mm representing group B. For group A implants, the maximum principal strain in the surrounding bone was 0.045; for group B implants, the maximum principal strain obtained was 0.015.

RESULTS

Insertion Torque Measurements

The installation torques were measured during the complete installation cycle and are illustrated in Figure 2. The differences in installation torque between groups A, B, and C are caused by different levels of condensation and different conditions of the respective sites. During ITQ measurement, four different regions can be identified. In region 1 (below 3.5 seconds), ITQ increases due to the fact that the bone is cut to match the outer shape of the implant. In region 2 (below 3.5–6 seconds), ITQ decreases since the bone profile matches the outer shape of the cutting region before the transition region starts. In the regions 1 and 2, the ITQ for the same site are identical regardless of test or control since the transition region has not reached the bone. In region 3 (6–10 seconds), the transition region gradually increases the strain level and installation torque for the test implants. The control implants exhibit no increase in ITQ. In region 4 (above 10 seconds), the condensation region equalizes the strain over the cortex and the installation torque is elevated for the test implants. If the implant is cutting threads in the apical bone at the end of implant installation, the torque increases slightly. This is in agreement with the earlier study.[8] The Maximum ITQ in region 4 is assumed to represent the initial stability.

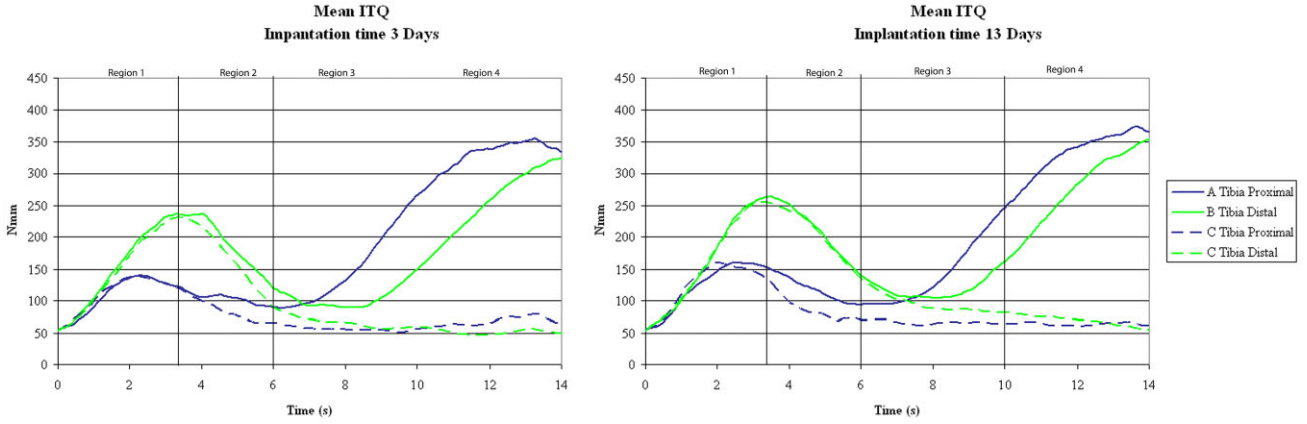

Figure 2 Mean ITQ values over time at installation. The differences in installation torque between group A, B, and C are caused by different levels of condensation and different sites. In the beginning, below 6 seconds, no condensation has occurred and, consequently, test and control have similar behavior in ITQ for respective sites.

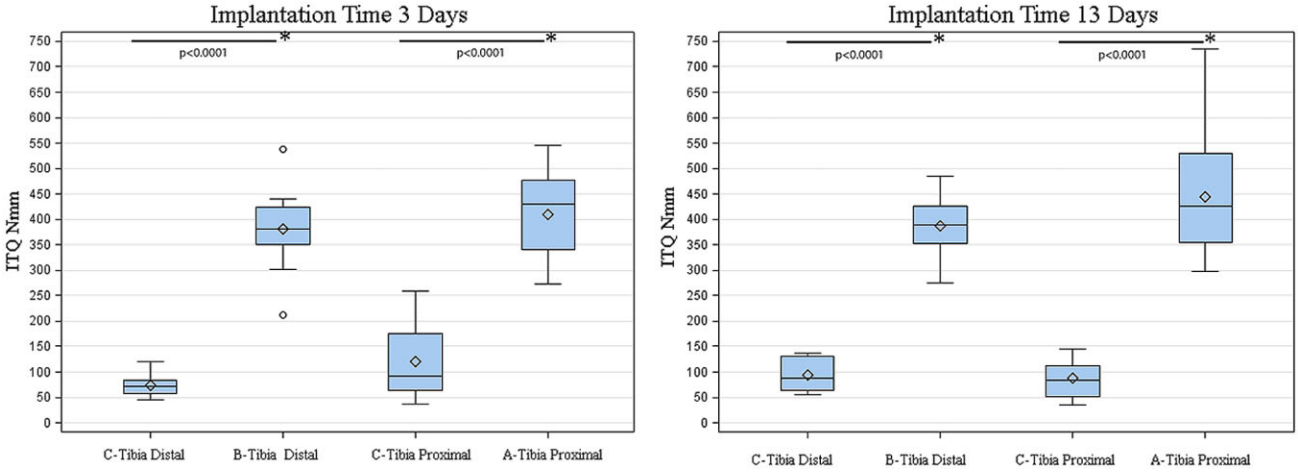

Figure 3 Box plot of the maximum ITQ values for two different implantations times. Group C has no condensation, group B has a moderate-level condensation, and group A has a high level of condensation. The asterisk means significant difference between test and control.

The results and the statistical analyses from the ITQ measurement for the two different implantation times 3 and 13 days and the three different implants (group A, group B and group C) are presented in a box plot (Figure 3 and Table 1). The difference in ITQ between test and control for 3 and 13 days of implantation times was normally distributed. The ITQs for group A and group B implants for 3 days implantation time were significantly higher than for the corresponding control group C ($p < .0001$ and $p < .0001$, respectively) and the ITQs for group A and group B implants for 13 days of implantation time were significantly higher than for the corresponding control group C ($p < .0001$ and $p < .01$, respectively).

RTQ Measurements

The results and the statistical analysis of the maximum RTQ measurement for the two different implantation times 3 and 13 days and the three different implants (group A, group B and group C) are presented in a box plot (Figure 4 and Table 2). The difference in RTQ between test and control for 3 and 13 days implantation times can be assumed to be normally distributed. The RTQs for group A and B at 3 days of implantation time were significantly higher than for the corresponding control group C ($p = .008$ and $p < .0001$, respectively), and the RTQs for group A and B at 13 days of implantation time were significantly higher than for the corresponding control group C ($p = .0005$ and $p = .0001$, respectively). The statistical analysis of the maximum RTQ value for three different implantation times (3, 13, and 24 days, the 24 days data are extracted from the previous study) is presented in Figure 6.

The RTQ for group A, B, and C, distal placement for 3, 13 and 24 days, can be assumed to be normally distributed. Group A exhibited no significant difference in

TABLE 1 Results from ITQ Measurement

Installation torque (ITQ)							
			Test		Control		
Implantation Time (Days)	Site	# Samples	Group	Mean Torque Nmm (SD)	Group	Mean Torque Nmm (SD)	*p*-Value *t*-Test
3	Tibia Prox	12	A	411 (91)	C	121 (76)	<.0001
3	Tibia Dist	12	B	381 (79)	C	73 (22)	<.0001
13	Tibia Prox	8	A	445 (128)	C	88 (38)	<.0001
13	Tibia Dist	8	B	387 (65)	C	94 (31)	<.0001

Due to the increased condensation, the ITQ for test implants were significantly higher compared to the control implants with no condensation.

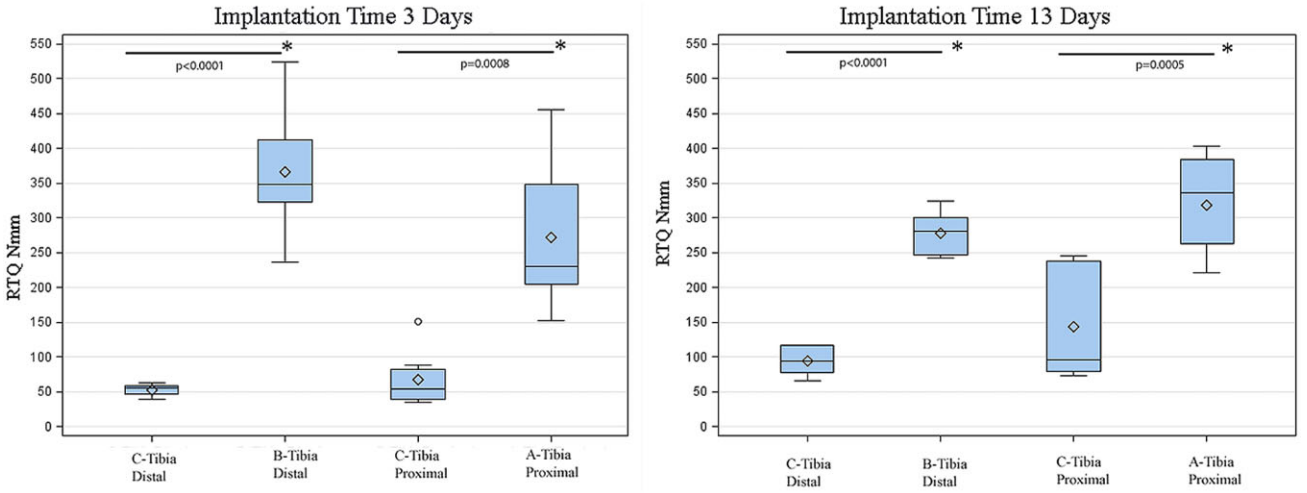

Figure 4 Removal torque for two different implantation times. Group C has no condensation, group B has a moderate-level condensation, and group A has a high level of condensation. The asterisk means significant difference between test and control.

RTQ between 3 and 13 days and 13 and 24 days ($p = .326$ and $p = .092$, respectively). For group B, there is a significant decrease in RTQ between 3 and 13 days and 13 and 24 days ($p = .024$ and $p = .046$, respectively). For group C, distal placement, there is a significant increase in RTQ between 3 and 13 days and 13 and 24 days ($p < .001$ and $p < .001$, respectively). The data for group C, proximal placement, can not be assumed to be normally distributed; therefore, no statistical analysis was performed. However, the RTQ seems to have increased over time.

Histomorphometry

Four sections had to be excluded since the condensed threads were not placed in the correct position. Therefore, the group C implants placed in the distal tibia at 3 days had to be excluded from the analysis due to only one measurement (Table 3). The remaining numbers of observations were insufficient to assume normally distributed data, and perform statistical analyses; however, the bone is in close contact with the implants for all groups (Figure 7) and there is a trend that the BIC is increased for the test implants compared to control implants (Table 3).

DISCUSSION

The present study investigated how insertion torque and RTQ after 3 and 13 days of implantation time are affected by two different magnitudes of static strain. In this study, implants in group A create an initial static strain of 0.045, which is beyond the ultimate strain (~0.02) of cortical bone and group B creates an initial static strain of 0.015 which is between the yield strain (~0.007) of cortical bone and ultimate strain (~0.02) of cortical bone.[13–15] The results obtained in this study indicate that the implantation site seems to have an

TABLE 2 Results from RTQ Measurement

			Removal Torque (RTQ)				
			Test		Control		
Implantation Time (Days)	Site	# Samples	Group	Mean Torque Nmm (SD)	Group	Mean Torque Nmm (SD)	*p*-Value *t*-Test
3	Tibia Prox	8	A	272 (104)	C	67 (39)	.008
3	Tibia Dist	8	B	366 (86)	C	53 (8)	<.0001
13	Tibia Prox	7	A	318 (66)	C	144 (77)	.005
13	Tibia Dist	7	B	278 (31)	C	94 (20)	<.0001

Due to the increased condensation, the RTQ for test implants were significantly higher compared to the control implants with no condensation.

TABLE 3 Results from Histologic Analysis

Histology							
		Test			Control		
Implantation Time (Days)	Site	Group	BIC (μm)	# Samples	Group	BIC (μm)	# Samples
3	Tibia Prox	A	420	4	C	366	3
3	Tibia Dist	B	443	4	C	–	1
13	Tibia Prox	A	560	4	C	429	3
13	Tibia Dist	B	436	4	C	284	4

The BIC for test implants seems higher compared to the control implants with no condensation.

impact on the installation torque (Figure 2). The observed differences in ITQ between the sites may be caused by site-specific properties. As expected, the development of the ITQ during the first 5–7 seconds was similar for the test and control implants at the two surgical sites which indicate no differences between the left and right leg (Figure 2). The present study investigated how the RTQ after 3 and 13 days of implantation in a rabbit model is affected by different static strains. Our previous study investigated how the RTQ is affected by the same induced strains after 24 days in rabbits.[8] Combining the RTQ data from the current study after 3, 13 days of implantation time with the data from the previous study after 24 days of implantation time,[8] the change of RTQ over time can be studied (Figure 5 and Figure 6). After 3 and 13 days of implantation, the RTQ for the test implants in this study was significantly higher than for the corresponding controls. This indicates that the press fit is maintained during the observed period. Similar findings were obtained after 24 days implantation. Group A exhibited no significant change over time, while group B had a significant decrease in RTQ over time. Group C, distal placement, had a significant increase in RTQ over time. There may be several explanations to these findings, but it may be suggested that: The change in RTQ values over time reflects the changes in prestress caused by two major components: 1) viscoelastic stress relaxation of the bone, and 2) biological activities such as 2a) modeling of bone at the implant bone interface (reducing bone) and 2b) remodeling by which prestressed bone is replaced by non-prestressed new bone. In an earlier study, in which Perren and colleagues[10] investigated how bone reacts to compression of an osteotomized site, it was found that the pressure dropped more rapidly during the first two weeks after which the pressure decreased linearly over time. It was stated that a resorption of only 10–20 μm at the osteotomy would have resulted in a completely

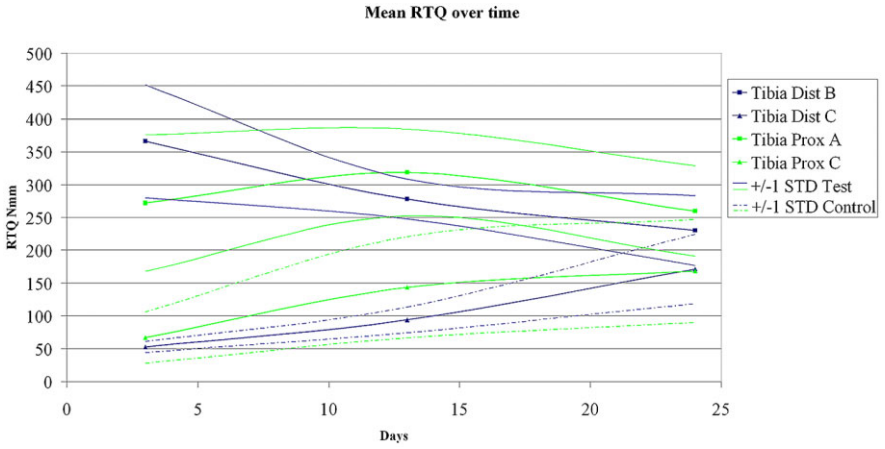

Figure 5 Change in RTQ over time with ±1 STD limit. Group A implants (Tibia Prox) induce high static strain in the bone, group B implants (Tibia Dist) induce moderate static strain, and group C implants (Tibia Prox/Dist) induce no static strain. The 3 and 13 days data are from the present study and the 24 days data are from Halldin and colleagues.[8]

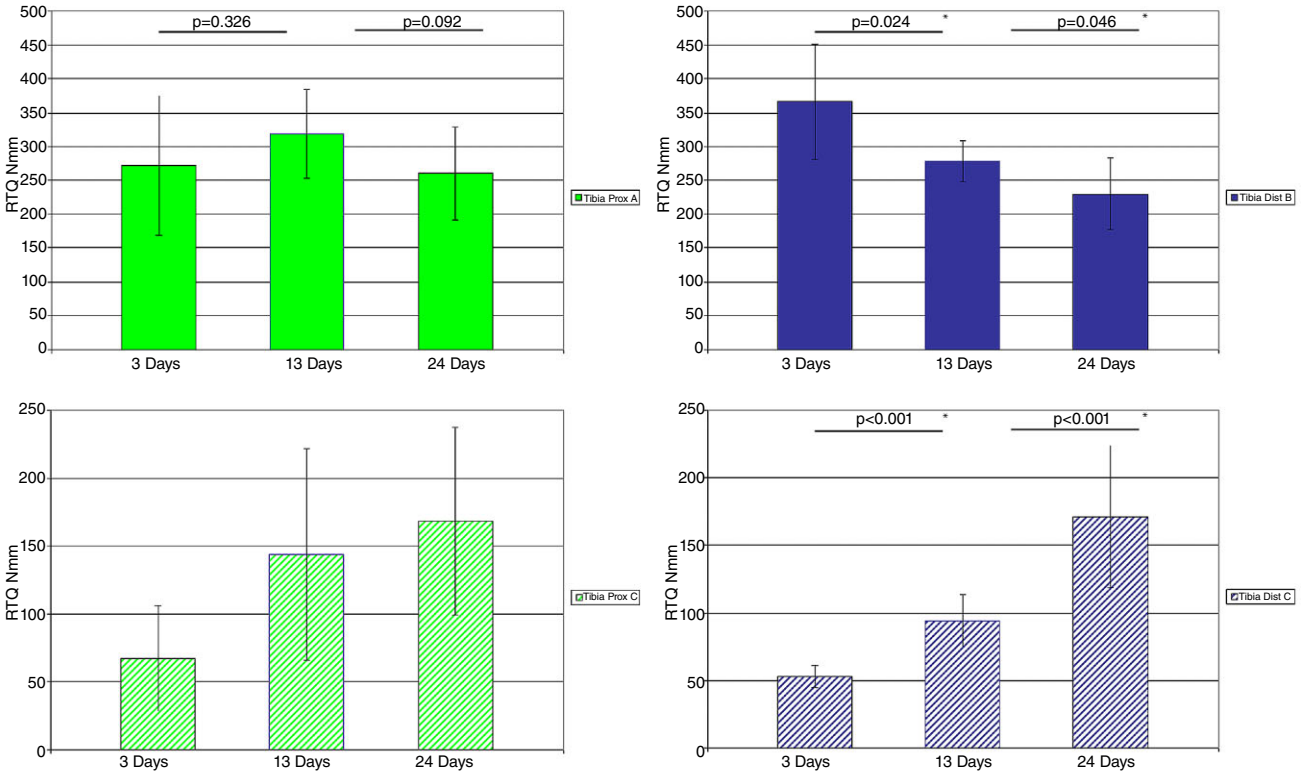

Figure 6 Statistical analysis of the changes in RTQ over time with corresponding p value. Group A implants (Tibia Proximal) induce high static strain in the bone. Group B implants (Tibia Distal) induce moderate static strain while group C implants (Tibia Proximal/Distal) induce no static strain. There is no change in RTQ over time for group A but a statistically significant decrease in RTQ over time for group B. Group C Dist had an statistically significant increase in removal torque over time. Group C Prox cannot be assumed to be normal distributed, but there is a tendency of increased RTO over time. The error bar represent ± one standard deviation. Asterisks represent significant difference. 3 and 13 days data are from the present study and 24 days data are from Halldin and colleagues.[8]

eliminated pressure. They suggested that viscoelastic stress relaxation was the predominant factor responsible for the decrease in prestress during the first two weeks, after which the reduction in prestress mainly was due to bone remodeling where prestressed bone is slowly replaced by non-prestressed bone.

For the group A implants, there was no statistically significant change in RTQ over time. Implants in group A produced a static strain far beyond the ultimate strain of cortical bone which may create microcracks in the bone (Figure 7). Zioupos and colleagues[26] analyzed the microdamage with different loading rates in a human femur and found that microcraking increases with strains beyond the yield strain, and it is assumed to be similar in rabbit bone. It may be speculated that the appearance of microcracks reduces the degree of strain, and therefore diminishes the effect of viscoelastic stress relaxation on RTQ. Other studies have suggested that microcracks or microdamage provoke bone remodeling.[27–29] The absence of statistically significant decrease in RTQ for group A implants between 3 and 13 days and 13 and 24 days may be a result of early bone formation in combination with diminished viscoelastic stress relaxation due to microcracks or microdamage. For the group B implants, inducing a static strain below the ultimate strain, there was a significant decrease in RTQ over time (Figure 6). Between 3 and 13 days for the group B implants, it is suggested that the predominant factor in the reduction of the prestress is viscoelastic stress relaxation. The results are similar to those of earlier studies[10,22] (Figure 6). Cortical bone remodels in a sequence of Activation-Resorption-Formation (A-R-F) by Basic Mulitcelluar Units (BMU).[30–32] BMU remodels bone at a rate of 20–40 µm/day and are approximately 0.2 mm wide.[31,33] Garetto and colleagues[34] found that bone adjacent to implants had high remodeling rate. The total turnover rate of bone remodeling is dependent on the number of active BMUs. Slaets and colleagues[32] studied the early cellular responses in cortical bone adjacent to an implant with undefined

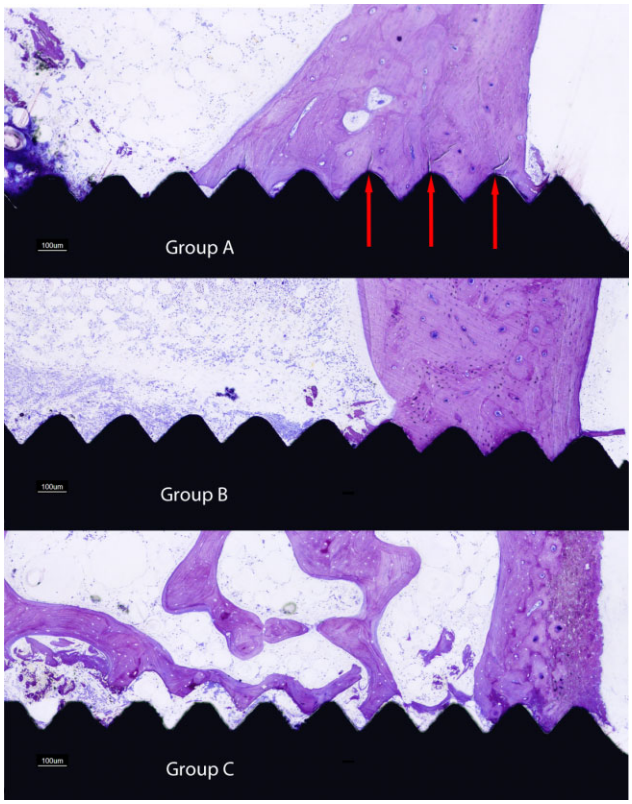

Figure 7 Histological images of test implants (group A and B) and control implants (group C proximal placement) after 3 days of implantation times. The bone is in close contact with the implants for all groups, but there is a tendency that the BIC is increased for the test implants (group A and B) regardless of implantation time compared to the control implants (group C). Cracks are visible for some of the sections in group A (red arrows) which induces high static bone strain. For group B, cracks were more difficult to detect.

press fit. It was found that the number of basic multicellular units were unchanged during the first 2 weeks, and then increased to be maintained on an elevated level 4–6 weeks after implant insertion. The delayed increase in the number of BMUs observed in Slaets and colleagues study may be interpreted as a lag time required for the BMU to be activated before remodeling is initiated. Roberts and colleagues[35] suggested that the activation time for rabbit cortical bone remodeling is approximately 0.5 weeks, which is less than what Slaets and colleagues[32] observed. In a study by Perren and colleagues,[10] approximately 7–12 days after initiated compression in sheep tibia, the pressure decreased linearly with time, which coincides with the elevated BMU activity in the study by Slaets and colleagues.[32] The linear reduction in pressure observed by Perren and colleagues[10] may be interpreted as once the BMUs are activated, the number of BMUs is constant until the prestressed bone has been replaced by non-prestressed bone. During bone modeling, formation and resorption occur independently of each other in contradiction to remodeling.[36] Bone formation at the bone-implant interface enhances the stability of the implant, and bone resorption at the bone-implant interface reduces the stability. Little is known about resorption rate of the bone at the bone-implant interface. Schulte and colleagues[37] measured the resorption rate using a newly developed computed tomography (CT) technique and found that for an unloaded mouse vertebra, the resorption rate was 0.15 μm/day. Martin and Buckland-Wright[38] developed a mathematical model and compared it to in vitro data to simulate the resorption depth and found that 3 days was required to resorb 22 μm of bone (~7.3 μm/day). Shimizu and colleagues[39] found that rabbit osteoclasts resorbed bone to a pit depth of 12.4 μm in mice after 60 hours (~5 μm/day) and in devitalized bone to a pit depth of 4.3 μm. The total resorption rate depends on the number of active osteoclasts and the rate of resorption of the individual osteoclast at the interface. In the current study, it is difficult to determine the number of osteoclasts at the bone-implant interface. However, it would require a large amount of osteoclasts to rapidly eliminate the complete press fit induced by group B implants (25 μm). Furthermore, there was a tendency of increased BIC for the test implants (groups A and B) compared to control implants (group C), indicating that higher condensation may not affect the bone resorption initially. Although not measurable from the sections, it may be speculated that only a few osteoclasts are present at the bone-implant surface and thus initially having a marginal affect on the RTQ. Similar findings were observed in the study by Perren and colleagues.[10] In the beginning, new bone consists of unmineralized osteoid which has a low mechanical strength and stiffness.[40] This bone gives a limited contribution to the RTQ value. During the osseointegration process, the newly formed bone increased in strength due to mineralization and due to remodeling from woven bone to lamellar bone which should lead to higher RTQ value. In the present study, the RTQ value for the control implants increases due to this process. The test implant in group B exhibited a decrease in RTQ over time. An explanation for this might be that in this case, the decrease in RTQ value caused by stress relaxation and possible bone resorption overrides the effect of osseointegration. In the present study, the decrease in RTQ may be explained as a

combined effect of bone stress relaxation, bone resorption, and bone remodeling. Directly after the implant is placed, the predominant factor in the reduction in RTQ is probably viscoelastic stress relaxation. Since revascularization of a condensed bone takes some time, resorption and remodeling require additional time to affect the RTQ.

CONCLUSIONS

This study indicates that increased static bone strains do not effect an extensive bone resorption but in addition to providing increased installation torque also provides an increased RTQ at 3 and 13 days after implant installation. The implant stability generated with moderate strain decreases over time and the implant stability generated with excessive strain is maintained over time.

ACKNOWLEDGMENTS

This work was supported by the Swedish Research Council (621-2010-4760).

We would like to acknowledge the assistance of Ms. Petra Johansson and Ms. Maria Hoffman for the animal surgery and sample preparation, Mr. Stefan Johnsson at Astra Tech for preparing all implants, and Mattias Sundén at Statistikkonsulterna Jostat and Mr. Sample for the statistical calculations.

REFERENCES

1. Cullen DM, Smith RT, Akhter MP. Bone-loading response varies with strain magnitude and cycle number. J Appl Physiol (Bethesda, Md.: 1985) 2001; 91:1971–1976.
2. Goodship AE, Lanyon LE, McFie H. Functional adaptation of bone to increased stress. An experimental study. J Bone Joint Surg Am 1979; 61:539–546.
3. Mosley JR, Lanyon LE. Strain rate as a controlling influence on adaptive modeling in response to dynamic loading of the ulna in growing male rats. Bone 1998; 23:313–318.
4. Qin YX, Rubin CT, McLeod KJ. Nonlinear dependence of loading intensity and cycle number in the maintenance of bone mass and morphology. J Orthop Res 1998; 16:482–489.
5. Rubin CT, Lanyon LE. Regulation of bone formation by applied dynamic loads. J Bone Joint Surg Am 1984; 66:397–402.
6. Rubin CT, Sommerfeldt DW, Judex S, Qin Y. Inhibition of osteopenia by low magnitude, high-frequency mechanical stimuli. Drug Discov Today 2001; 6:848–858.
7. Turner CH, Owan I, Takano Y. Mechanotransduction in bone: role of strain rate. Am J Physiol 1995; 269:E438–E442.
8. Halldin A, Jimbo R, Johansson CB, et al. The effect of static bone strain on implant stability and bone remodeling. Bone 2011; 49:783–789.
9. Lynch JA, Silva MJ. In vivo static creep loading of the rat forelimb reduces ulnar structural properties at time-zero and induces damage-dependent woven bone formation. Bone 2008; 42:942–949.
10. Perren SM, Huggler A, Russenberger M, et al. The reaction of cortical bone to compression. Acta Orthop Scand Suppl 1969; 125:19–29.
11. Gibson LJ. The mechanical behaviour of cancellous bone. J Biomech 1985; 18:317–328.
12. Reilly DT, Burstein AH. Review article. The mechanical properties of cortical bone. J Bone Joint Surg Am 1974; 56:1001–1022.
13. Currey JD. Tensile yield in compact bone is determined by strain, post-yield behaviour by mineral content. J Biomech 2004; 37:549–556.
14. McCalden RW, McGeough JA, Barker MB, Court-Brown CM. Age-related changes in the tensile properties of cortical bone. The relative importance of changes in porosity, mineralization, and microstructure. J Bone Joint Surg Am 1993; 75:1193–1205.
15. McElhaney JH. Dynamic response of bone and muscle tissue. J Appl Physiol 1966; 21:1231–1236.
16. Cochran DL. The evidence for immediate loading of implants. J Evid Based Dent Pract 2006; 6:155–163.
17. Stanford CM. Surface modification of biomedical and dental implants and the processes of inflammation, wound healing and bone formation. Int J Mol Sci 2010; 11:354–369.
18. Bashutski JD, D'Silva NJ, Wang HL. Implant compression necrosis: current understanding and case report. J Periodontal Res 2009; 80:700–704.
19. Norton MR. The influence of insertion torque on the survival of immediately placed and restored single-tooth implants. Int J Oral Maxillofac Implants 2011; 26:1333–1343.
20. Isaksson H, Malkiewicz M, Nowak R, Helminen HJ, Jurvelin JS. Rabbit cortical bone tissue increases its elastic stiffness but becomes less viscoelastic with age. Bone 2010; 47:1030–1038.
21. Lakes RS, Katz JL, Sternstein SS. Viscoelastic properties of wet cortical bone – I. Torsional and biaxial studies. J Biomech 1979; 12:657–678.
22. Cordey J, Blumlein H, Ziegler W, Perren SM. Study of the behavior in the course of time of the holding power of cortical screws in vivo. Acta Orthop Belg 1976; 42(Suppl 1):75–87.
23. Johansson CB, Jimbo R, Stefenson P. Ex vivo and in vivo biomechanical test of implant attachment to various materials: introduction of a new user-friendly removal torque equipment. Clin Implant Dent Relat Res 2010; 14:603–611.

24. Donath K, Breuner G. A method for the study of undecalcified bones and teeth with attached soft tissues. The Sage-Schliff (sawing and grinding) technique. J Oral Pathol 1982; 11:318–326.
25. Johansson CB, Morberg P. Importance of ground section thickness for reliable histomorphometrical results. Biomaterials 1995; 16:91–95.
26. Zioupos P, Hansen U, Currey JD. Microcracking damage and the fracture process in relation to strain rate in human cortical bone tensile failure. J Biomech 2008; 41:2932–2939.
27. Bentolila V, Boyce TM, Fyhrie DP, Drumb R, Skerry TM, Schaffler MB. Intracortical remodeling in adult rat long bones after fatigue loading. Bone 1998; 23:275–281.
28. Burr DB, Martin RB, Schaffler MB, Radin EL. Bone remodeling in response to in vivo fatigue microdamage. J Biomech 1985; 18:189–200.
29. Mori S, Burr DB. Increased intracortical remodeling following fatigue damage. Bone 1993; 14:103–109.
30. Frost HM. From Wolff's law to the Utah paradigm: insights about bone physiology and its clinical applications. Anat Rec 2001; 262:398–419.
31. Parfitt AM. Osteonal and hemi-osteonal remodeling: the spatial and temporal framework for signal traffic in adult human bone. J Cell Biochem 1994; 55:273–286.
32. Slaets E, Carmeliet G, Naert I, Duyck J. Early cellular responses in cortical bone healing around unloaded titanium implants: an animal study. J Periodontol 2006; 77:1015–1024.
33. Albrektsson T. Repair of bone grafts. A vital microscopic and histological investigation in the rabbit. Scand J Plast Reconstr Surg 1980; 14:1–12.
34. Garetto LP, Chen J, Parr JA, Roberts WE. Remodeling dynamics of bone supporting rigidly fixed titanium implants: a histomorphometric comparison in four species including humans. Implant Dent 1995; 4:235–243.
35. Roberts WE, Turley PK, Brezniak N, Fielder PJ. Implants: bone physiology and metabolism. J Calif Dent Assoc 1987; 15:54–61.
36. Roberts WE, Huja S, Roberts J. Bone modeling: biomechanics, molecular mechanisms, and clinical perspectives. Semin Orthod 2004; 10:123–161.
37. Schulte FA, Lambers FM, Kuhn G, Muller R. In vivo micro-computed tomography allows direct three-dimensional quantification of both bone formation and bone resorption parameters using time-lapsed imaging. Bone 2011; 48:433–442.
38. Martin MJ, Buckland-Wright JC. Sensitivity analysis of a novel mathematical model identifies factors determining bone resorption rates. Bone 2004; 35:918–928.
39. Shimizu H, Sakamoto M, Sakamoto S. Bone resorption by isolated osteoclasts in living versus devitalized bone: differences in mode and extent and the effects of human recombinant tissue inhibitor of metalloproteinases. J Bone Miner Res 1990; 5:411–418.
40. White AA 3rd, Panjabi MM, Southwick WO. The four biomechanical stages of fracture repair. J Bone Joint Surg Am 1977; 59:188–192.